

REDUCTION OF UNSTEADY WIND TORQUES
ON AN OPEN PORT AIRBORNE OPTICAL TURRET

by

John P. Thomas, Jr., Lt, USAF

and

James T. Van Kuren, PhD

I. INTRODUCTION

The use of an aero/optics system on an aircraft during flight requires the development of a pointing and tracking assembly for the telescope. This optical system is normally contained within a turret assembly, of which two major types are pre-eminent. Figures 1 and 2 contain diagrams of these two designs, which are called the "on-gimbal" and "Coelostat" turrets, respectively. A major feature of these turrets is the open port optical cavity. At the present time most aero/optics applications require the use of a cavity open to the free stream of the airflow about the turret in flight.

The turrets are designed to allow rotation of the entire system about the central axis, plus rotation of an inner gimbal containing the cavity and telescope about an axis perpendicular to the central axis of symmetry. These two types of rotation, called rotations in azimuth and elevation, respectively, are depicted in Figure 3. The drive mechanisms which induce these rotations must overcome the steady and unsteady wind torques caused by the airflow about the turret. The "on-gimbal" turret shown in Figure 1 utilizes "inner" and "outer" drive mechanisms. The outer drives are powerful devices intended for large angular rotations of the entire turret, whereas the inner drives control only the inner gimbal of the turret and provide the fine adjustment to the telescope system. The torque capacities of the inner drives are much lower than those of the outer mechanisms. In particular, the unsteady wind torques, acting on the inner gimbal portion of the turret must be minimized if this drive system is to perform as desired.

The objective of this paper is to present techniques for reducing the unsteady torques acting on the inner gimbal of a turret of the types shown in Figures 1 and 2. The reductions in the unsteady torques are obtained by using "fixes" that alter undesirable flow characteristics or change the acoustic properties of the turret cavity. These "fixes" are designed to be used in the subsonic and transonic flow regimes. The flow field about the turret is generally three-dimensional and turbulent, and shock waves can form because of the rapid acceleration of the compressible gas about the blunt turret. The situation is further complicated by the presence of the cavity flow, and the fact that the mouth of the cavity must sweep through a wide angular variation relative to the direction of the freestream. The extreme complexity of this flow situation has precluded an analytical approach to the problem. Instead, several experimental investigations have been conducted by the Air Force and NASA to obtain aerodynamic torque data and to attempt various methods for reducing torque unsteadiness on turrets of the types described earlier. A 3/10 scale open port turret test was conducted in the NASA Ames 14 T Wind Tunnel facility in January - February 1972. Although the primary emphasis of this test was to consider various shapes fore and aft of the turret to minimize drag and buffet, some progress was made towards turret inner gimbal unsteady torque reduction. It was determined that significant reductions of the unsteady pressures measured in the turret cavity could be obtained by the use of porous wind screens around the aperture of the cavity mouth. The use of these wind screens was motivated in part by some previous results presented in Reference 1. A subsequent test at Ames from September-November 1972 considered the problem of unsteady torque reduction in much greater detail, with a

variety of methods considered. Much of the results obtained in this test are described in an unpublished Air Force Weapons Laboratory document (Reference 2). A synopsis of the test results were presented in an AIAA paper (Reference 3), but a detailed description of these methods of torque reduction has not appeared in the open literature. The intention of the present work is to present in a fairly detailed manner the effectiveness of the various approaches to torque reduction, with particular emphasis on the comprehensive results of the second Ames test noted above.

II. MECHANISMS OF FLOW INDUCED UNSTEADY TORQUE GENERATION

It is essential that an understanding of the primary mechanisms of flow induced unsteady torque generation be achieved before a rational approach can be made to the methods of reduction of this torque. As a consequence, this section will include a brief account of the primary features of the flow about the turret and cavity which are thought to contribute significantly to the magnitude of the unsteady wind torque.

The most basic aspect of the flow that suggests a source of unsteady torques is the well known phenomenon of the excitation of cavity resonance by airflow. Analytical work in this area began with the classical efforts of Helmholtz and Rayleigh (Reference 4). More recently, notable experimental efforts to study cavity flow have been conducted by Roshko (Reference 5), Dunham (Reference 6), and others. A simplified model of the flow situation is obtained if one considers the shear layer across the mouth of the cavity as a region of instability resulting from the presence of inflection points in the velocity profile. Dunham (Reference 6) references some unpublished smoke tunnel work by Brown and Quinn that includes photographs and high speed motion pictures. This and other work indicates that the inflection points and pressure gradient in the flow across the mouth of the cavity results in vortices which eventually strike the downstream lip of the cavity. (See Figure 4) When these vortices satisfy the condition

$$f_i = \frac{nUe}{L_s} \quad (2.1)$$

where n is an integer number of vortices in the shear layer, Ue is the velocity of the vortices along the shear layer, L_s is the length of the shear layer over the cavity, and f_i is the frequency of the i th resonant mode of the cavity, then the cavity is said to be in resonance. The coupling of the cavity oscillations with the flow induced forcing functions tends to further contribute to the magnitude of the oscillations. The existence of a resonance condition in the cavity is a major contributor to unsteady, periodic torques on the inner gimbal of the turret.

It is evident from this brief discussion of flow induced cavity resonance that two separate approaches may be taken to diminish the effects of this problem. Either the shear layer over the mouth of the cavity must be modified so that the layer is stabilized or moved out of the cavity, or the cavity itself must be altered so that it dampens the propagation of the acoustic disturbances. The various methods employed at the NASA Ames tests mentioned earlier and elsewhere have included the use of porous wind screens around the cavity opening, variation of the radius of the lip of the cavity, the injection of air into the cavity through a porous cylindrical insert, the injection of air through slots around the cavity lip, inserts of various porosity used

as the cylindrical walls of the cavity, and the insertion of dense foam liners of several compressibilities and thicknesses along the cavity walls. It is evident from the extent of the effort in this area that the problem of cavity resonance is considered to be the major contributor to the torque unsteadiness that can be alleviated by relatively simple methods.

It should be recognized that cavity resonance is not the only cause of unsteady torques on the inner gimbal of the turret. It has already been mentioned that shock waves can form on the turret, even at relatively low Mach numbers ($M_\infty > 0.55$). These shock waves can interact with the turret boundary layer in an unstable and often periodic manner. Pressure fluctuations can propagate through the subsonic boundary layer and provide a further input to the cavity pressure fluctuations. The turret is also subject to the shedding of vortices in the wake, which provides a periodic side force to the turret. A description of this type of vortex shedding may be found in Reference 7. A large variety of fairings of various designs have been used to alleviate both the problem of vortex shedding and to lower the drag levels on the turret. The size of the fairings is limited due to the desirability of a large field of view for the turret. Tests such as the ones previously mentioned at NASA Ames have indicated that the fairings have little effect on the unsteady pressures inside of the cavity at transonic speeds. However, results given in Reference 8 indicate that at subsonic Mach numbers less than about $M_\infty = 0.55$ the presence of the fairing can have a dramatic effect on the cavity unsteady pressures. These effects seem to be negligible at all Mach numbers higher than $M_\infty = 0.55$. Since most applications of these optical turrets involve Mach numbers in the transonic range, the low Mach number pressure effects of the fairings will not be of concern here. Results presented in this work will therefore be for a single turret/fairing combination.

III. INSTRUMENTATION, MODEL AND TEST DETAILS

It has been previously mentioned that the bulk of the Air Force/NASA effort in unsteady torque reduction took place during the wind tunnel test at the Ames 14T facility in the autumn of 1972. In this section further details of the experimental set-up and instrumentation used in this test are presented.

The NASA Ames 14 Foot Wind Tunnel facility is a closed-circuit, atmospheric facility. The basic turret and fairing model used in the test was mounted on a splitter plate that was 3.74 meters long by 1.37 meters wide. This splitter plate was mounted to a side wall of the tunnel on six 1.14 meter legs (See Figure 5). The Advanced Pointer Tracker (APT) turret was remotely driven in azimuth and elevation. Although this turret was tested with a variety of fairings, the only combination considered in the present work is that shown in Figure 6.

The measurement of the unsteady inner gimbal torques was accomplished using appropriately located high response pressure transducers. Twenty-eight locations were chosen to provide the contributions to the unsteady torques about the inner gimbal axes of the APT turret. Each instrumentation location was considered to be the centroid of a representative area. The resulting nondimensionalized torque

coefficients were obtained using the following equation:

$$C_T = \frac{\sum_{i=1}^{28} p_i A_i r_i}{q_{\infty D}^3} \quad (3.1)$$

where q_{∞} was the freestream dynamic pressure. D was the turret diameter, p_i was the i th unsteady pressure. A_i was the i th area associated with a pressure, and r_i was the moment arm of the i th pressure location about the appropriate axis. As noted earlier, the use of Equation (3.1) to obtain the nondimensionalized torques neglects the effects of skin friction. The unsteady pressure signals were summed on a real-time basis to determine the unsteady torque signal. Figure 7 indicates the locations of unsteady pressure transducers inside the cavity of the turret.

The first of the various types of "fixes" used were the external wind screens (EWS). The typical geometry of these screens is represented in Figure 8. These screens were all constructed from sheet metal perforated with circular holes of uniform distribution which provided a range of porosity from 10% to 37%. The heights of these screens varied from 0.63 cm to 2.53 cm above the surface of the turret. The screens were cylindrical in shape, with the central axis coincident with the telescope axis. Two varieties of screens were tested - the other EWS had a diameter of 25.7 cm, which corresponded to a ratio of screen to aperture diameter of 1.275, whereas the inner EWS diameter equaled the aperture diameter of 20.1 cm. For some tests, spacers were placed under the EWS's to provide a gap between the surface of the turret and the screen.

Various types of inserts were used to provide acoustic treatment of the internal walls of the cavity. These "internal wind screens" (IWS) (Figure 9) corresponded to an aperture diameter of 20.1 cm. In some cases, simple sheet metal with circular holes to provide 10% to 30% porosity were tried. During other test runs porous plastic foam of various thicknesses was placed over the IWS's. Foam with acoustic impedances of 20 to 60 rayls/cm were experimented.

The configuration of the tip of the cavity was expected to influence cavity resonance. Three lip radii were tried to determine separation and re-attachment interactions with the cavity. The three radii were 0 (sharp lip), 0.76 cm and 1.71 cm.

Another approach to resonance suppression was the injection of air through the 37% porous IWS or through slots along the cavity lip (Figure 10). For the latter, the lip was split into two 180° segments connected to separately controlled air lines.

IV. EXPERIMENTAL RESULTS

The various configurations were compared under similar test conditions. Elimination of resonance and a reduction of r_{ms} pressures, forces and torques were used to determine the effectiveness of the various antiresonant devices.

Effect of Fairings. Vortex shedding from the blunt turret seemed to be a source of noise for the cavity. Practically any kind of aft fairing or splitter and a low forward fairing reduced the opportunity for cross communication of pressure waves and therefore reduced the RMS pressures in the cavity at subsonic speeds below Mach number 0.55. At higher Mach numbers the low interference fairing (Figure 6) had only slightly reduced pressure fluctuations. These results were encouraging enough that development of fairings continued to the point of the present Airborne Laser Laboratory Cycle III fairings.

Effects of Porous Fences. The lip fences (external wind screens) had two effects on the open cavity and shell; one was favorable. Figure 11 shows that considerable reduction in rms pressure could be achieved by increasing the height of a 50% porous fence. The improvement occurred regardless of transducer position and was attributed to increased shear layer thickness over the opening. The unfavorable effect was that the fences had relatively high aerodynamic drag which was transmitted to the shell as external torque (Figure 12). Solid and 30% porous fences were also tested. Evaluation of all of the data, including that not shown in this paper, lead to the conclusion that a 30% porous fence with height (h) approximately 1/16 of the cavity diameter (D) was a satisfactory compromise (Figure 12).

Effect of Lip Radius. Three lip radii were tried during the tests. The lowest RMS torques and pressures were obtained with a sharp lip (Figure 13). The output was very sensitive to transducer position but unsatisfactorily high in all cases. As shown on the figure, the addition of the lip fence reduced the rms pressures considerably.

Effect of Cavity Inserts. A solid cavity side wall (cylindrical), one with 10% porosity (equally spaced circular holes), and a 37% porous wall were investigated. Plastic foam liners were subsequently added to the solid wall as another approach at pressure reduction. Increased porosity reduced rms pressure (Figure 14) at all transducer locations. The foam proved to be even more beneficial. Figure 15 is plotted in terms of rms torques and shows the large reductions to be obtained with low density foam.

Discussion. Considering the open cavity in an unprotected shell with minimal fairings as a base line, the best combination tested with mechanical fixes was a shell with a low interference fairing, a 1/16 h/D 30% porous lip fence around a sharp lip, and low density sidewall insert. The effect of this configuration on dynamic pressure and internal torque was significant (Figure 16). RMS pressures were reduced by the best configuration to about 1% of the dynamic pressure, values normally sensed for boundary layer turbulence. The steady azimuth and elevation torques were also reduced to negligible values for "side look" arrangements. However, for determining the size of the positioning servo motors for telescope gimbals, it is necessary to know what the maximum unsteady loads would be. At any given Mach number, the maximum load occurs at some different combination of azimuth and elevation angles. These maxima increase in value with Mach number, so the attempts to reduce loads should be concentrated at the highest Mach number of the application. Though not shown on the figures, a torque reduction of approximately 50% at $M = 0.9$ between protected and unprotected cavities was realized in this study.

Effect of Mass Injection. Gaseous mass injection was found to be a significant new method of reducing resonance in open port cavities. Resonance occurred at certain azimuth angles resulting in large values of rms torque (Figure 16). Injection of gas through the pores in the 37% internal insert resulted in reductions in unsteady pressure and torque below the best mechanical configuration. The flow rate of gas required is related to the size of the opening and the mass flux ($\text{kg/m}^2 \text{ sec}$) of the free stream air. For flight applications it is necessary to minimize the gas flow. Injection of the air through a narrow slit on the upstream edge of the opening produced a reduction in the required mass flow rate by approximately 50%.

V. CONCLUSIONS AND RECOMMENDATIONS

The occurrence of acoustic resonance and internal torque in open cavities on blunt protuberances is dependent on Mach number, Reynolds number and the angle of the plane of the opening relative to the free stream direction.

Several techniques were investigated for reducing the unsteady pressures and torques.

Fairings are necessary to protect the external shell from excessive loads, and have a beneficial effect on internal pressures.

A lip fence with 30% porosity and height equal to 1/16 the cavity diameter reduced rms pressures by an order of magnitude and reduced torques by 50%.

Porous cavity walls of 37% reduced the overall unsteady pressure levels by 30% to 60% depending on the location of the transducer. Low density foam likewise reduced unsteady internal torques by an order of magnitude.

Injection of air over the opening was more efficiently done with a thin slot on the upstream lip. Maximum torques were reduced 75% by this technique.

In summary, it is recommended that a combination of configurations be used for protecting an open port optical system from steady and unsteady aerodynamic loads in an airborne environment. Dynamic surface pressures can be maintained at levels similar to those experienced from boundary layer turbulence.

REFERENCES

1. Buell, D. A., "An Experimental Investigation of the Airflow over a Cavity with Anti-Resonance Devices," NASA TN D6205 (1971).
2. Davis, J. A., "Investigation of the 0.3-Scale Open Port APT Turret at NASA Ames 14T: Phase II," unpublished AFWL TR (1974).
3. Van Kuren, J. T., "Acoustic Phenomena of Open Cavity Airborne Cassegranian Telescopes," AIAA Paper No. 74-195 (1974).
4. Rayleigh, J. W. S., "The Theory of Sound," Mac Millan Co., Ltd., Vol. 2, pp. 412-414, 170-235 (1896).
5. Roshko, A., "Some Measurements of Flow in a Rectangular Cutout," NACA TM 3488 (1955).
6. Dunham, W. H., "Flow-Induced Cavity Resonance in Viscous Compressible and Incompressible Fluids," Office of Naval Research, ACR-92 (1962).
7. Roshko, A., "Structure of Turbulent Shear Flows: A New Look," AIAA Journal, Volume 14, pp. 1349-57 (1976).
8. Thomas, J. P. Jr., "Test of Turret/Fairing Configurations for the B-52 SRAT Program," AFFDL-TM-FXM-79-21 (1979).

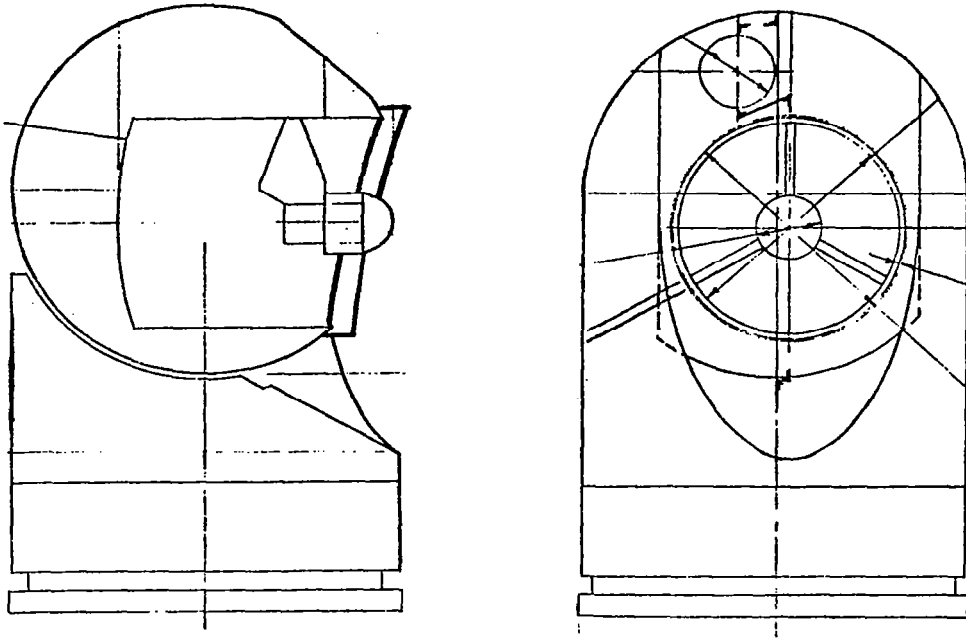


FIGURE 1. ON-GIMBAL TURRET.

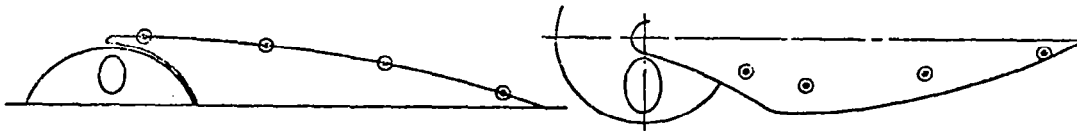


FIGURE 2. COELOSTAT TURRET.

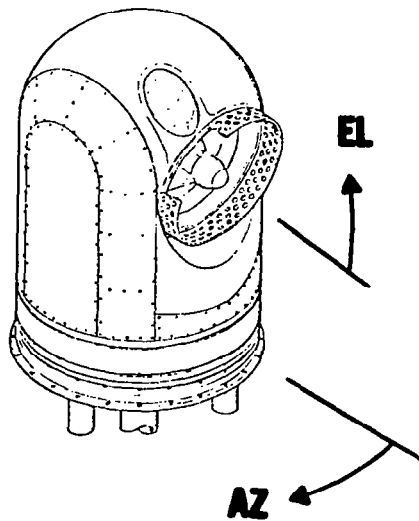


FIGURE 3. AZ AND EL ANGLES.

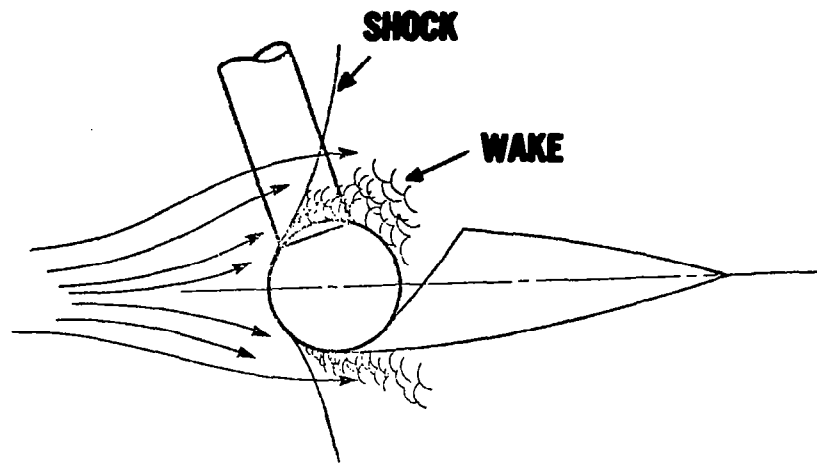


FIGURE 4. FLOW FIELD AT CAVITY MOUTH.

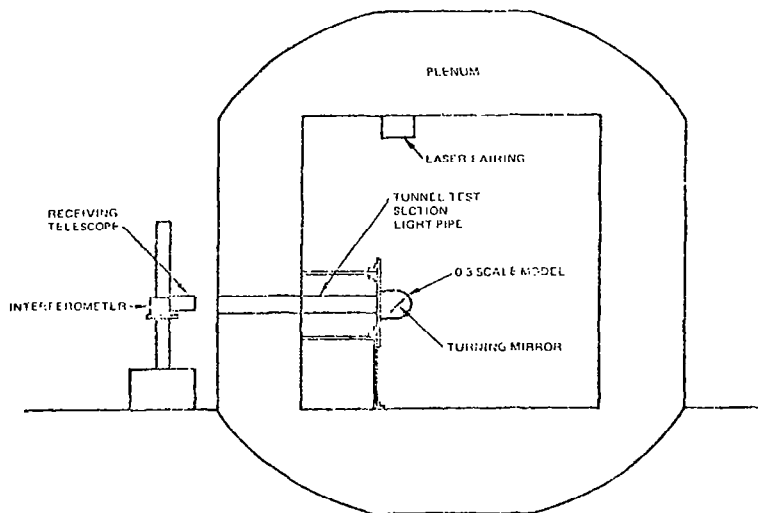


FIGURE 5. MODEL MOUNTED TO TUNNEL WALL.

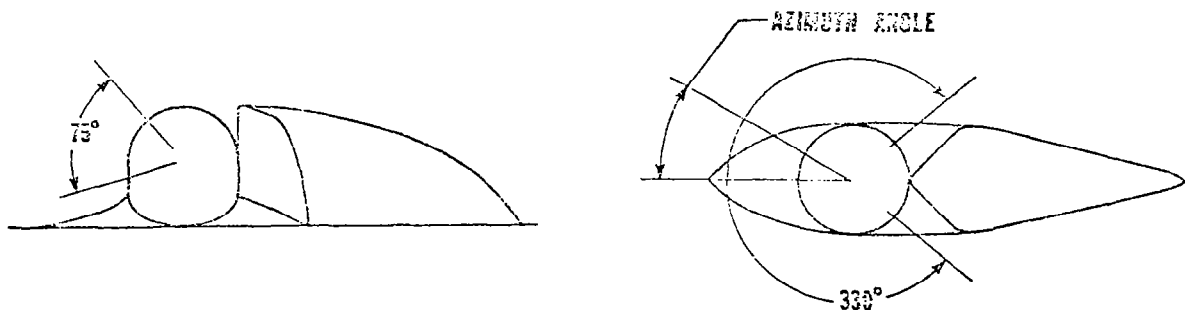
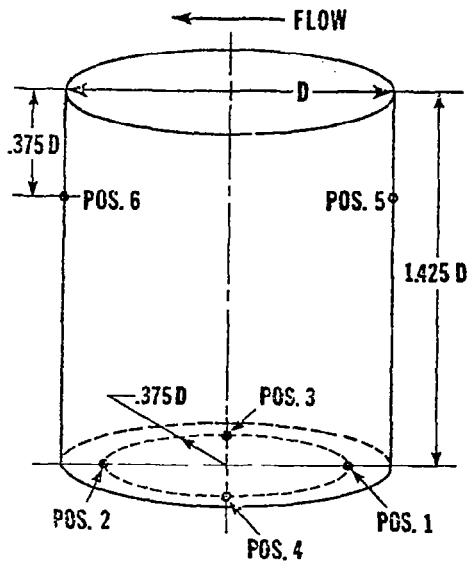
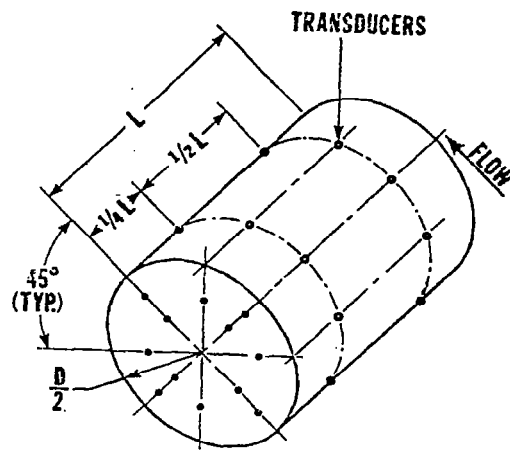


FIGURE 6. NON-INTERFERENCE FAIRING.

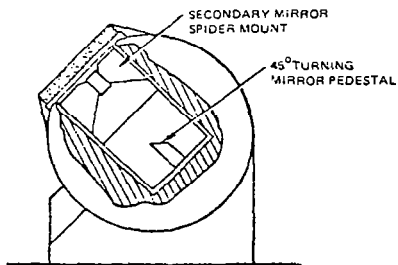


TRANSDUCER NOTATION

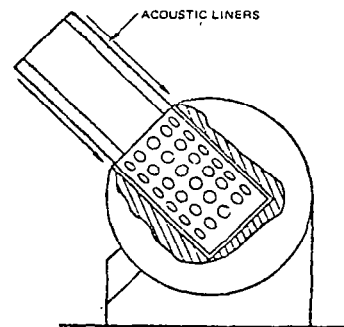


CAVITY INSTRUMENTATION
(FOR OBTAINING TORQUES)

FIGURE 7. TRANSDUCER LOCATIONS.



EXTERNAL WIND SCREENS
(SOLID, 30% POROSITY,
50% POROSITY)



FULL INSERTS
(SOLID, 10% POROSITY,
AND 37% POROSITY)

FIGURE 8. EXTERNAL WIND SCREEN.

FIGURE 9. INTERNAL WIND SCREEN.

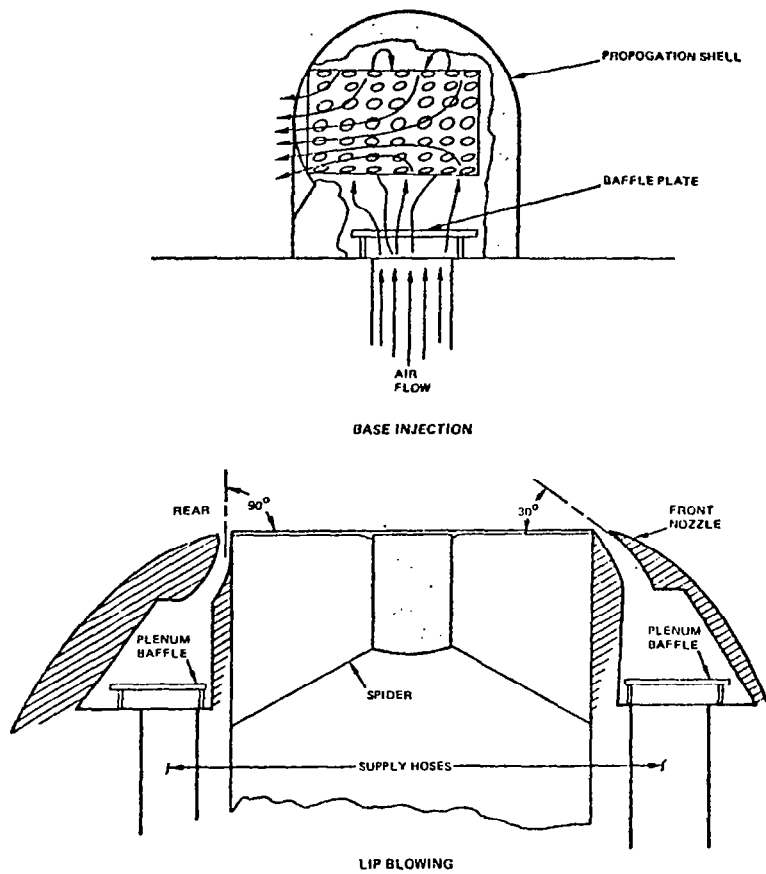


FIGURE 10. TECHNIQUES FOR AIR INJECTION.

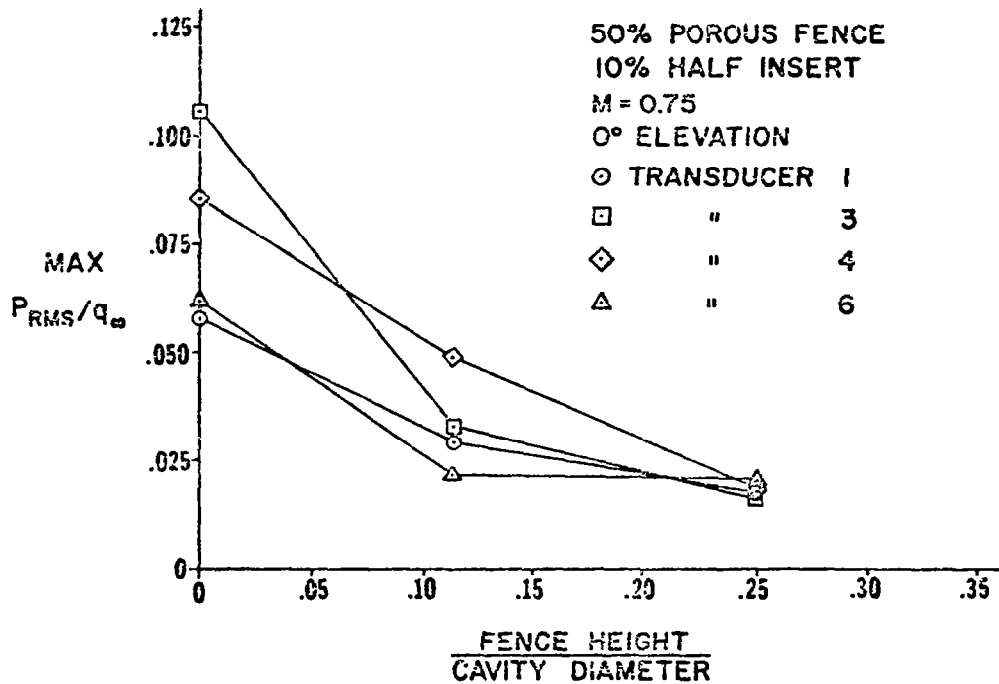


FIGURE 11. LIP FENCE HEIGHT VS CAVITY UNSTEADY PRESSURES.

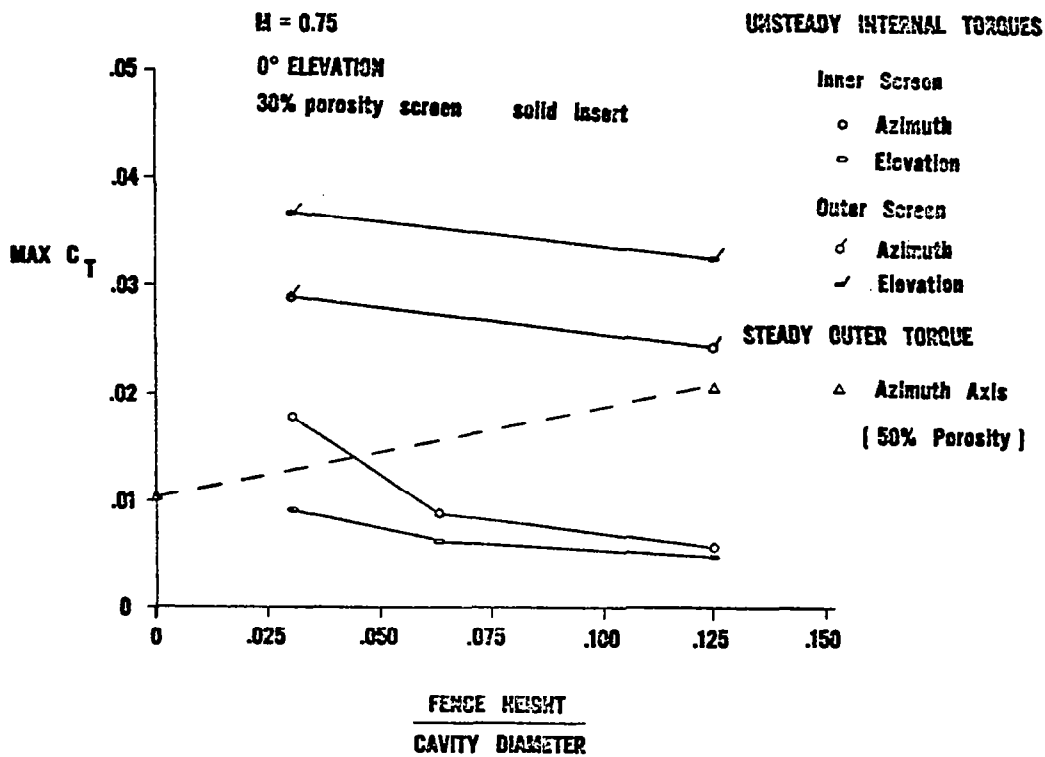


FIGURE 12. LIP FENCE HEIGHT VS UNSTEADY AZIMUTH TORQUES.

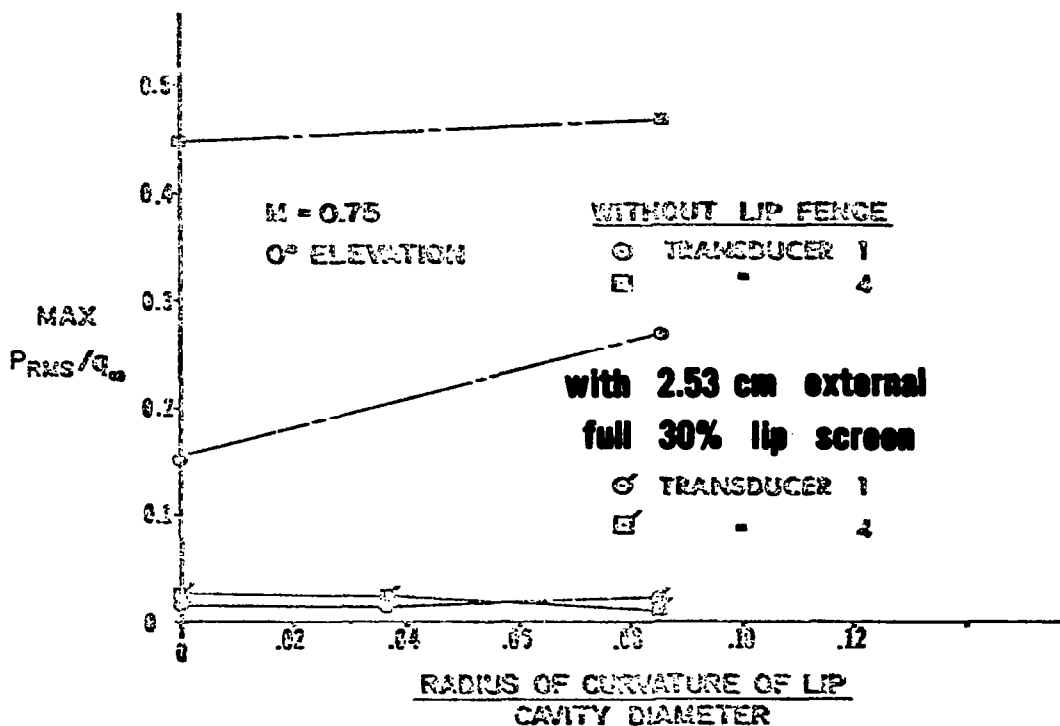


FIGURE 13. CAVITY LIP RADIUS VS CAVITY UNSTEADY PRESSURES.

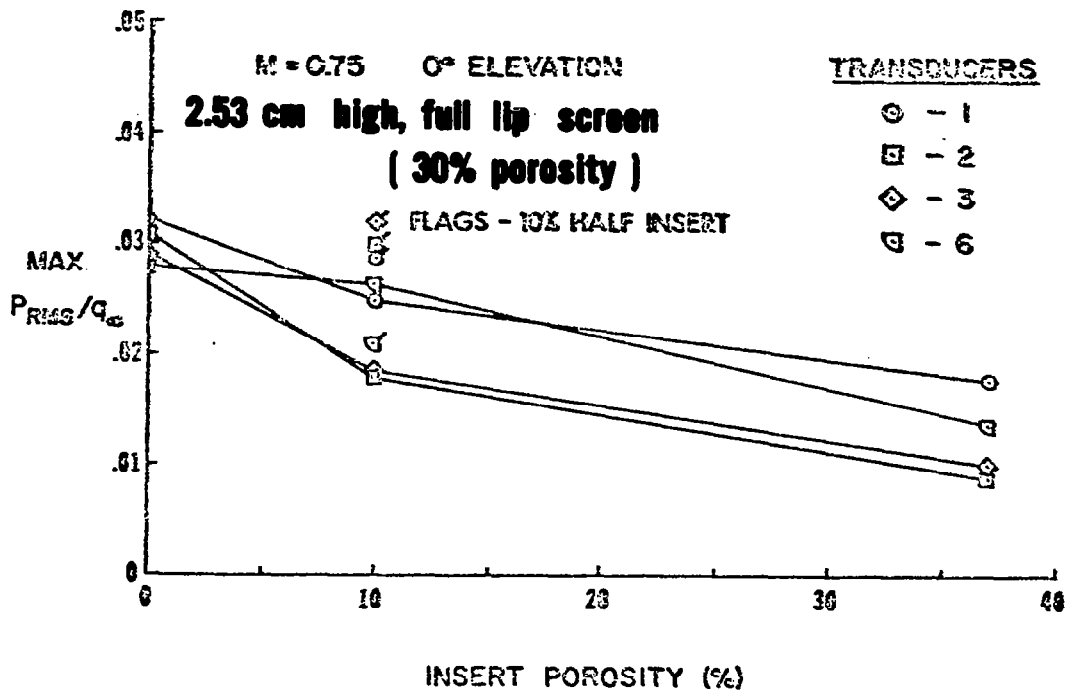


FIGURE 14. INSERT POROSITY VS CAVITY UNSTEADY PRESSURES.

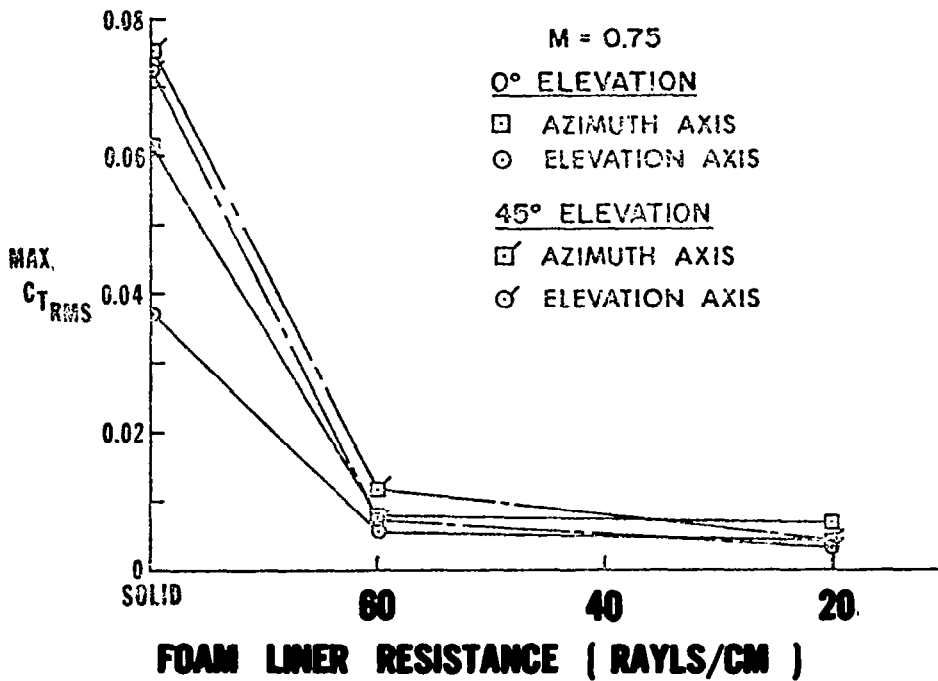


FIGURE 15. INSERT POROSITY VS UNSTEADY AZIMUTH TORQUES.

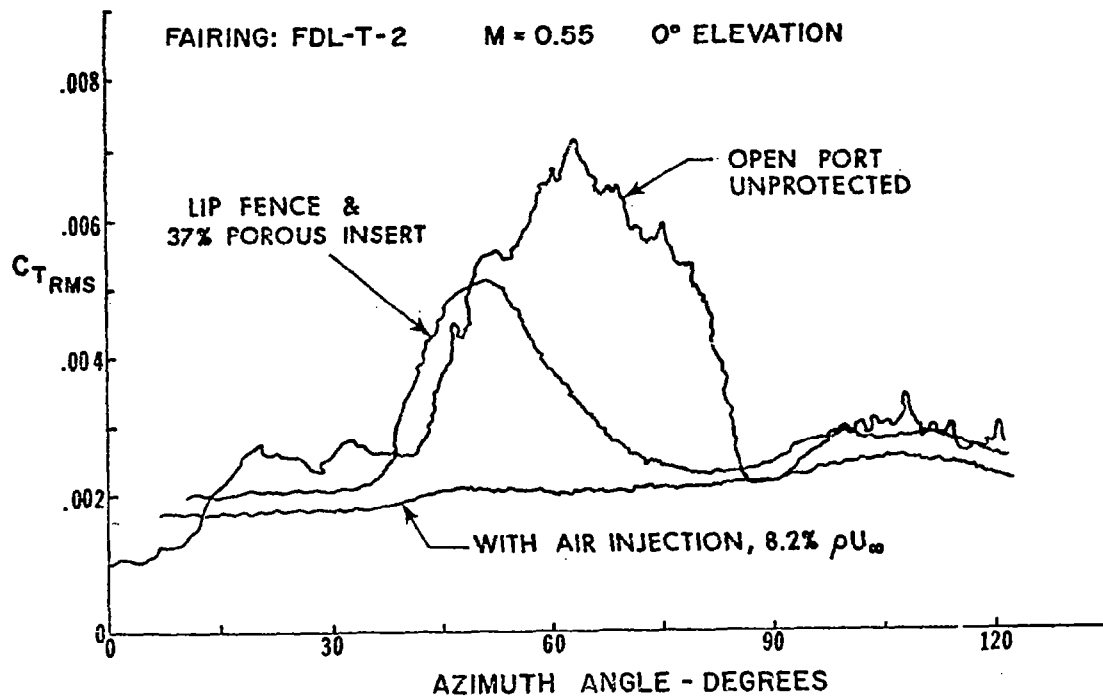


FIGURE 16. UNSTEADY AZIMUTH TORQUE COMPARISONS.